A peer-reviewed version of this preprint was published in PeerJ on 27 October 2016.

View the peer-reviewed version (peerj.com/articles/2595), which is the preferred citable publication unless you specifically need to cite this preprint.

Tanaka KH, Vincent AT, Trudel MV, Paquet VE, Frenette M, Charette SJ. 2016. The mosaic architecture of *Aeromonas salmonicida* subsp. *salmonicida* pAsa4 plasmid and its consequences on antibiotic resistance. PeerJ 4:e2595 https://doi.org/10.7717/peerj.2595

The mosaic architecture of *Aeromonas salmonicida* subsp. *salmonicida* pAsa4 plasmid and its consequences on antibiotic resistance

Katherine H Tanaka, Antony T Vincent, Mélanie V Trudel, Valérie E Paquet, Michel Frenette, Steve J Charette

Aeromonas salmonicida subsp. *salmonicida*, the causative agent of furunculosis in salmonids, is an issue especially because many isolates of this bacterium display antibiotic resistances, which limit treatments against the disease. Recent results suggested the possible existence of alternative forms of pAsa4, a large plasmid found in *A. salmonicida* subsp. *salmonicida* and bearing multiple antibiotic resistance genes. The present study reveals the existence of two newly detected pAsa4 variants, pAsa4b and pAsa4c. We present the extensive characterization of the genomic architecture, the mobile genetic elements and the antimicrobial resistances genes of these plasmids in addition to the reference pAsa4 from the strain A449. The analysis showed differences between the three architectures with consequences on the content of resistance genes. The genomic plasticity of the three pAsa4 variants could be partially explained by the action of mobile genetic elements like insertion sequences. Isolates from Canada and Europe that bore similar antibiotic resistance patterns than pAsa4-bearing strains were genotyped and specific pAsa4 variants could be attributed to phenotypic profiles. pAsa4 and pAsa4c were found in Europe, while pAsa4b was found in Canada. The plasticity of pAsa4 variants related to the acquisition of antibiotic resistance indicates that these plasmids may pose a threat in terms of the dissemination of antimicrobial-resistant *A.salmonicida* subsp. *salmonicida* bacteria.

PeerJ Preprints | https://doi.org/10.7287/peerj.preprints.2067v1 | CC-BY 4.0 Open Access | rec: 23 May 2016, publ: 23 May 2016

The mosaic architecture of *Aeromonas salmonicida* subsp. *salmonicida* pAsa4 plasmid and its consequences on antibiotic resistance

Katherine H. Tanaka[1,2,3], Antony T. Vincent[1,2,3], Mélanie V. Trudel[1,2,3], Valérie E. Paquet[1,2,3], Michel Frenette[2,4], and Steve J. Charette[1,2,3]

[1]Institut de Biologie Intégrative et des Systèmes (IBIS), Université Laval, Quebec City, Quebec, Canada

[2]Département de biochimie, de microbiologie et de bio-informatique, Faculté des sciences et de génie, Université Laval, Quebec City, Quebec, Canada

[3]Centre de recherche de l'Institut universitaire de cardiologie et de pneumologie de Québec, Quebec City, Quebec, Canada

[4]Groupe de Recherche en Écologie Buccale (GREB), Faculté de médecine dentaire, Université Laval, Quebec City, Quebec, Canada

Corresponding author:

Steve J. Charette[1,2,3]

Institut de Biologie Intégrative et des Systèmes (IBIS), 1030, Avenue de la Médecine, Quebec City, Québec, Canada, G1V 0A6

E-mail: steve.charette@bcm.ulaval.ca

Abstract

Aeromonas salmonicida subsp. *salmonicida*, the causative agent of furunculosis in salmonids, is an issue especially because many isolates of this bacterium display antibiotic resistances, which limit treatments against the disease. Recent results suggested the possible existence of alternative forms of pAsa4, a large plasmid found in *A. salmonicida* subsp. *salmonicida* and bearing multiple antibiotic resistance genes. The present study reveals the existence of two newly detected pAsa4 variants, pAsa4b and pAsa4c. We present the extensive characterization of the genomic architecture, the mobile genetic elements and the antimicrobial resistances genes of these plasmids in addition to the reference pAsa4 from the strain A449. The analysis showed differences between the three architectures with consequences on the content of resistance genes. The genomic plasticity of the three pAsa4 variants could be partially explained by the action of mobile genetic elements like insertion sequences. Isolates from Canada and Europe that bore similar antibiotic resistance patterns than pAsa4-bearing strains were genotyped and specific pAsa4 variants could be attributed to phenotypic profiles. pAsa4 and pAsa4c were found in Europe, while pAsa4b was found in Canada. The plasticity of pAsa4 variants related to the acquisition of antibiotic resistance indicates that these plasmids may pose a threat in terms of the dissemination of antimicrobial-resistant *A. salmonicida* subsp. *salmonicida* bacteria.

PeerJ Preprints | https://doi.org/10.7287/peerj.preprints.2067v1 | CC-BY 4.0 Open Access | rec: 23 May 2016, publ: 23 May 2016

Introduction

The ubiquitous waterborne Gram-negative bacterium *Aeromonas salmonicida* subsp. *salmonicida* is the causative agent of furunculosis, a disease that affects aquaculture operations worldwide (Derome et al. 2016). The main treatments for this disease are vaccination and antibiotics. Vaccination was shown to be efficient but is expensive and may cause major side effects (Dallaire-Dufresne et al. 2014). Antibiotics are becoming increasingly less effective against *A. salmonicida* subsp. *salmonicida* due to the spread of antibiotic resistance genes. For example, more and more antibiotic-resistant *A. salmonicida* subsp. *salmonicida* strains are being isolated and characterized, many of them bearing resistance genes on plasmids (McIntosh et al. 2008; Piotrowska & Popowska 2015; Sorum et al. 2003; Vincent et al. 2014b).

In *A. salmonicida* subsp. *salmonicida*, insertion sequences (ISs) are responsible for several genomic modifications (Vincent et al. 2016). ISs are made of a transposase gene and inverted repeats. Their high number in psychrophilic *A. salmonicida* increases the risk of composite transposon formations, recombinations, deletions and inversions (Vincent et al. 2016). Some ISs are involved in virulence loss when *A. salmonicida* subsp. *salmonicida* is under stressful conditions (IS*AS1*, IS*AS2* and IS*AS11*) (Gustafson et al. 1994; Tanaka et al. 2012). Furthermore, many plasmid variants display transpositions or IS-mediated recombinations when compared to their reference (IS*AS*5 in many plasmids, IS*Ec*9 in pSN254b) (Attere et al. 2015; Najimi et al. 2009; Trudel et al. 2013; Vincent et al. 2014b). Given the high number of ISs in the genome of this bacterium (Studer et al. 2013; Vincent et al. 2016), as well as their presence in most associated genomic entities, we hypothesize that ISs play a role in plasmid reshaping (Tanaka et al. 2013).

63

64 The large plasmid pAsa4 from *A. salmonicida* subsp. *salmonicida* carries resistance genes that
65 provide resistance against chloramphenicol, spectinomycin, streptomycin, sulfonamides,
66 tetracycline, mercury, and quaternary ammonium compounds (Reith et al. 2008). Except for
67 tetracycline resistance, these genes are located in Tn*21*, a non-composite transposon. Tn*21* is a
68 widespread replicative transposon that also carries another mobile element, the integron In*2*
69 (Liebert et al. 1999). The complete sequence of pAsa4 was first described in reference strain
70 A449, which originated from France (Reith et al. 2008). Genotyping done in a previous study has
71 shown that some *A. salmonicida* subsp. *salmonicida* isolates likely bear pAsa4 but do not display
72 the expected antibiotic resistance profile (Vincent et al. 2014b). This suggests that pAsa4
73 variants may have evolved from a common replicon backbone, but do not share the same
74 antibiotic resistance genes.

75

76 We used next-generation sequencing (NGS) on two isolates, one from the province of Quebec
77 (Canada) and one from Switzerland, suspected of carrying pAsa4 variants based on preliminary
78 genotyping and antibiotic resistance profiles, to obtain the complete sequences of the two
79 plasmids. Both plasmids exhibited marked differences with the original pAsa4 plasmid from the
80 reference strain A449 and with each other. Mobile genetic elements such as ISs are involved in
81 some of these differences. Our results indicate that plasmid reshaping drives the antibiotic
82 resistance diversity of *A. salmonicida* subsp. *salmonicida* and may affect its ability to
83 disseminate this diversity.

Material and Methods

Bacterial isolates, growth conditions, and antibiotic resistance profiles

The *A. salmonicida* subsp. *salmonicida* strains listed in Table S1 were included in this study. All strains were grown on furunculosis agar (10 g of Bacto-Tryptone, 5 g of yeast extract, 1 g of L-tyrosine, 2.5 g of NaCl, and 15 g of agar per liter of distilled water) for two or three days at 18°C (Hanninen & Hirvela-Koski 1997). To complete the analyses done previously by Vincent and collaborators, disk diffusion assays were performed using the same protocol for strains listed in Table S1 in order to detect chloramphenicol (30 µg), florfenicol (30 µg), sulfamethoxazole/trimethoprim (SXT) (23.75 µg/1.25 µg), and tetracycline (5 µg) (Becton Dickinson, USA) resistances (Vincent et al. 2014b).

DNA extraction and sequencing

The total genomic DNA of two isolates (01-B522 and JF2267) was extracted using DNeasy Blood and Tissue kits (Qiagen, Canada) and was sequenced at the Plateforme d'Analyse Génomique of the Institut de Biologie Intégrative et des Systèmes (IBIS, Université Laval). Isolate 01-B522 was sequenced as previously described (454 GS-FLX+ technology, mate-pair library with 5 kbp fragment size and 1500 bp library size) (Vincent et al. 2014a). For JF2267, a 650-bp shotgun library was sequenced using 454 GS-FLX+ technology. The reads were assembled *de novo* using Newbler version 2.5.3 with default parameters (Margulies et al. 2005).

Sequence analysis

Contigs resulting from the assembly of 01-B522 and JF2267 were initially mapped locally on the sequence of the pAsa4 from A449 (GenBank accession number NC_009349.1) using CONTIGuator version 2.7.4 (Galardini et al. 2011). All contig junctions were manually verified by PCR and Sanger sequencing and links were joined using Consed version 27 (Gordon & Green 2013).

The assembled plasmids were annotated as follows. Briefly, open reading frames (ORFs) were predicted by getorf (available as a part of EMBOSS 6.6.0.0) (Rice et al. 2000). All the detected ORFs were then compared to pAsa4 coding sequences using fasta36 (Pearson & Lipman 1988). Lastly, the remaining ORFs were annotated using Blastn and Blastp (Altschul et al. 1990) against the NCBI non-redundant (nr/nt) database and, if necessary, against the whole genome shotgun database (wgs, Gammaproteobacteria (taxid:1236)). Annotations were manually verified using the Artemis version 16.0.0 visualization tool, and alignments between the assembled pAsa4 were visualized using EasyFig 2.1 and ACT 13.0.0 (Rutherford et al. 2000; Sullivan et al. 2011). Antibiotic resistance genes were validated with The Comprehensive Antibiotic Resistance Database (CARD) (McArthur et al. 2013). The annotated sequences of pAsa4b and pAsa4c were deposited in GenBank under accession numbers KT033469 and KT033470, respectively.

The average copy number per cell for pAsa4b in 01-B522 and pAsa4c in JF2267 were estimated by mapping the sequencing reads using TAPyR v1.3-beta4 (Fernandes et al. 2011) and by

128 calculating the average coverage using Qualimap 2.0 (Garcia-Alcalde et al. 2012). The copy
129 numbers were standardized against the average coverage of the *gyrB* housekeeping gene (single
130 copy per chromosome).
131
132 Contigs from two other *A. salmonicida* strains, RS 534 (NCBI wgs JYFF00000000) (Vincent et
133 al. 2016) and JF3517 (Attere et al. 2015) were mapped against pAsa4, pAsa4b, and pAsa4c using
134 CONTIGuator version 2.7.4.
135
136 A global alignment of pAsa4b and pAsa4c was performed using *stretcher* (available as a part of
137 EMBOSS 6.6.0.0) (Rice et al. 2000), and a custom R script (R Core Team 2015) was used to
138 visualize the number of substitutions by 1000-bp sliding windows (Data S1) (Zeileis &
139 Grothendieck 2005). For the heatmap representations, all the ORFs from pAsa4b were compared
140 to the NCBI nucleotide collection (nr/nt) using tBlastn (Altschul et al. 1990). The data was
141 ordered and visualized using a custom R script (Wickham 2009). k-means clustering was used to
142 group target sequence identifiers based on the matrix results in as many clusters that could create
143 reproducible grouping (Data S2) (Hartigan & Wong 1979).
144

145 ## PCR analyses

146 The DNA templates, PCR mixtures, and program cycles were performed as previously described
147 (Trudel et al. 2013), with the exception of the elongation time, which was 1 min per kbp of
148 amplicon. The PCR assays were performed at least twice, and appropriate positive and negative
149 controls were included with each assay. The PCR primers are listed in Table S2. Genotyping

150 primers were designed using PrimerBlast (Ye et al. 2012) at plasmid insertion/deletion sites
151 (junction between segments, Fig. 1B).
152

Results

Complete sequences of the new pAsa4 variants

A. salmonicida subsp. *salmonicida* isolate 01-B522 harbored a potential pAsa4 variant based on the genotyping results and antibiotic-resistance profile (Vincent et al. 2014b) (Table 1). Isolate JF2267 displayed genotyping results similar to those of 01-B522, but had a different antibiotic resistance profile (Table 1). To determine the complete sequences of these potential pAsa4 variants, NGS combined with PCR and Sanger sequencing were used to assemble the complete plasmid sequences. The reference plasmid pAsa4 is composed of 166,749 bp and 173 ORFs and has a G+C content of 52.8% (Reith et al. 2008) compared to 181,933 bp, 175 ORFs, and a G+C content of 52.48% for 01-B522 pAsa4 variant (pAsa4b), and 163,022 bp, 156 ORFs, and a G+C content of 53.42% for JF2267 variant (pAsa4c). Based on the relative coverage of the sequenced reads compared to *gyrB* coverage, the estimated number of copies of the pAsa4 variants in 01-B522 and JF2267 was 1 in both cases. The contigs alignments of strains RS 534 and JF3517 indicated that they had the same content as pAsa4 and pAsa4c, respectively.

pAsa4 and its variants bear many ORFs coding for hypothetical proteins (Fig. 1A, cyan arrows). The plasmids also carry ORFs for their replication and partition and for proteins with other functions (all shown in Fig. 1A as black arrows). Furthermore, two regions bear resistance antibiotic genes (Fig. 1A, orange arrows). Tn*21*, a transposon whose presence was already acknowledged in pAsa4, carry the most of resistance genes via its built-in integron, In*2* (Liebert et al. 1999; Reith et al. 2008). A tetracycline resistance gene and its repressor are located

175 elsewhere on the plasmid (Fig. 1A). Finally, the conjugation-related genes (Fig. 1A, blue arrows)
176 are separated in two loci.
177
178 Large insertions or deletions, as well as an inversion, have occurred between the pAsa4 variants,
179 as shown in the sequences alignment (Fig. 1A). These events have mainly occurred between each
180 plasmid first conjugative loci, Tn*21*s, and *tetA(E)* flanking sequences. Insertion sequences have
181 caused alignment gaps as well. Otherwise, the three pAsa4 variants displayed a high level of
182 sequence identity (from 94 to 99%) for syntenic regions, with pAsa4b being more similar to
183 pAsa4 than pAsa4c. Base substitution count by 1-kbp window between pAsa4b and pAsa4c
184 showed that some regions are more prone to mutations (Fig. S1). In fact, more than 50
185 substitutions per kilobase occurred upstream from the first transfer genes (Fig. 1B, start of
186 orange segment and Fig. S1 at 45-50 kbp) and in a long ORF only predicted in pAsa4c's first
187 conjugative block (Fig. 1A, longest hypothetical protein in this region and Fig. S1 at 72 kbp). On
188 the other hand, almost no mismatches were found in the 60-kbp region that comprised Tn*21* and
189 the region downstream from it (Fig. S1, between 125 and 165 kbp).
190

191 ## Insertion sequences

192 All pAsa4 variants carry insertions sequences (ISs) (Fig. 1A, named red arrows). pAsa4b and
193 pAsa4c retained the same IS types that were described in pAsa4, namely IS*AS1*, IS*AS2*, IS*AS5*
194 and IS*AS9* (Reith et al. 2008) (see also GenBank accession number NC_009349.1). However, no
195 IS shared the same location among all variants, except for the disrupted IS*AS5* nesting the Tn*21*
196 copy. In pAsa4 and pAsa4c, two different ISs (IS*AS9* and IS*AS2*, respectively) are inserted in
197 this disrupted IS (Fig. 1A, downstream of the transposon). In the case of pAsa4c, a new gene (a

198 putative acetyltransferase) had potentially co-transposed with IS*AS2* since it was only found in
199 association with IS*AS2* on pAsa4c (Fig. 1A, asterisk).
200
201 A comparison of transposase sequences using Blast and of inverted repeats using the IS Finder
202 database indicated that there was a member of the IS*1595*-family (Siguier et al. 2006) in pAsa4c
203 (Fig. 1A, dagger). This IS, IS*Kpn3*, has been originally identified in *Klebsiella pneumoniae*
204 plasmid pRDDHA (Verdet et al. 2006). To our knowledge, this was the first identification of this
205 IS in *A. salmonicida*. Based on the Blast search results against the NCBI nr/nt and wgs
206 databases, IS*Kpn3* is present in *Aeromonas* genus, namely in *Aeromonas media* WS plasmid
207 (accession number CP007567.1) and in *Aeromonas dhakensis* SSU strain (accession number
208 JDWD00000000.1).
209

210 ## Detailed plasmid architecture

211 We compared all three pAsa4's architecture to assess their impact on the plasmid function,
212 including antibiotic resistances (Fig. 1). To facilitate the analysis and the following genotyping,
213 syntenic regions among the variants were grouped together as empirical segments (Fig. 1B,
214 colored rectangles). We investigated the features in each segment as well as their boundaries to
215 infer the causes of these large-scale rearrangements.
216
217 A first segment (Fig. 1B, blue rectangle) contained an IS*AS2*, Tn*7*-like transposition protein
218 genes (ABCD), and tetracycline resistance genes (*tetAR*(E)). It was absent from pAsa4c
219 compared to pAsa4 and pAsa4b, which explains why JF2267 was not resistant to tetracycline
220 (Table 1). An imperfect 36-nucleotide repeated sequence flanking this segment in pAsa4 and

pAsa4b was not found in pAsa4c at the deletion site, suggesting that it could have been involved in the recombination-deletion process.

Tn*21* and its In*2* spawned over three segments based on this partition (Fig. 1B, yellow, pink and light green rectangles). Two contiguous variations in In*2* are comprised in one segment (Fig. 1B, pink rectangle) that differentiated pAsa4b from pAsa4c and pAsa4, the latters carrying identical integrons. pAsa4b In*2* bears the integrase, a fused cassette *qacE*Δ*1 sul1*, a putative acetyltransferase and *tniAB*Δ*3* (Fig. 2). pAsa4 and pAsa4c In*2* bear an additional *aadA* gene (synonym: *aadA1*) that codes for an aminoglycoside nucleotidyltransferase (ANT(3'')) (Ramirez & Tolmasky 2010). Also, the pAsa4b integron does not bear the *cat* gene (synonym: *catA1*, encoding a class A-1 chloramphenicol acetyltransferase) (Fig. 2). Accordingly 01-B522, which bears pAsa4b, is sensitive to chloramphenicol (Vincent et al. 2014b). However, this gene is not inserted as a cassette in In*2*. Instead, there was evidence of an IS*CR* insertion flanking the *cat* gene when it is present. IS*CR* use replicative rolling circle transposition to transpose (Toleman et al. 2006). This IS*CR* should bear the transposase and special structures (*ori*IS in 3' and *ter*IS in 5') that are essential for rolling circle replication. Based on gene identities and annotations, pAsa4 and pAsa4c have a partial transposase from an IS*CR* and an IS*CR* 3', but are lacking the other components (Fig. 2).

The regions in the three plasmids harboring most of the conjugative transfer genes also displayed the most differences (Fig. 1B, rainbow rectangles). An inversion of the *traELBVA* locus and the surrounding region seemed to have occurred in pAsa4. This inversion is flanked by two inverted IS*AS1*s, which are in the appropriate position to have mediated the rearrangement. Only one of

the two IS*AS1* was found at this position in pAsa4b, while both are absent in pAsa4c. However, several genes of unknown function upstream from the transfer locus were deleted from this position in pAsa4c. The two new variants also have an insertion contiguous to the *traELBVA* locus that is not present in pAsa4 (Fig. 1B, rainbow rectangle, green to purple). This region is slightly longer in pAsa4b and harbors other transfer genes and coding sequences. Interestingly, the ultimate downstream gene in this segment is a putative phage-type endonuclease that shares identity with a pAsa4 pseudogene that, given the inversion and deletion in this region, is at the same location with respect to the other coding sequences in pAsa4.

Comparative analysis of the pAsa4 architecture

A tBlastn search of pAsa4b coding sequences (excluding IS transposases) against the NCBI non-redundant database was achieved to collect 516 uniquely identified sequences that were hit more than three times. By *k-means* clustering, those sequences were reproducibly clustered into four groups, one of which had two sub-groups (Fig. 3). Overall, identity percentage for the hits was between 20 and 80%, except for Group 2, where the identity was near 100%. Group 1 was divided into sub-groups a and b, which would always be differentiated by the *k-means* analysis. Group 1 (Fig. 3, red and orange) had hits for coding sequences scattered along pAsa4b against the A/C_2 family conserved backbone (Fricke et al. 2009; Harmer & Hall 2015). pRA1, a A/C_1 plasmid, also fell in this category (Harmer & Hall 2015). The hits covered the majority of the plasmid, including the first and second conjugative block (Fig. 1A), but not the *tet* region (Fig. 1B, blue segment) nor the region directly downstream of IS*AS5*-Tn*21*. Group 2 (Fig. 3, green) had hits targeted at Tn*21*/In*2*. However, its sequence identifiers were more disparate. Group 3 (Fig. 3, purple) had hits against integrative conjugative elements (ICE) and the *Vibrio* STX-

pathogenesis island for some of the coding sequences that provided hits in Group 1. Group 4 (Fig. 2, blue) had more heterogeneous identifiers and had hits for more specific coding sequences, including sequences for the Tn*7*-like transposition proteins and the *hipAB* toxin-antitoxin genes.

A final alignment was performed between pAsa4b and another *A. salmonicida* subsp. *salmonicida* plasmid, pSN254b (Fig. 4). pSN254b is a large IncA/C_2 plasmid that is also found in Canadian isolates (Vincent et al. 2014b). The identity between continuous segments was between 59% and 81%, and the synteny between genes was well conserved, a feature that could not be analysed by the heatmap. Again, the *tet*-containing segment (Fig. 4, blue rectangle) and a region directly downstream from Tn*21* were not covered by the alignment (Fig. 4).

Variant genotyping and antibiotic resistances

Some insertions and deletions between pAsa4 variants changed their antibiotic resistance gene content. Consequently, A449, bears pAsa4 and exhibits resistance to tetracycline and chloramphenicol, JF2267 carries pAsa4c and displays resistance to chloramphenicol and 01-B522 bears pAsa4b and exhibits resistance to tetracycline and sulfamethoxazole-trimetoprim (SXT) (Table 1). All resistances but SXT, which is an antibiotic combination used in aquaculture (Morin 2010), are directly explained by their respective pAsa4 architecture. JF2267 tetracycline sensitivity is related to a segment deletion in pAsa4 that carry *tetA(E)* (Fig. 1B, blue segment). 01-B522 chloramphenicol sensitivity is explained by its In*2* structure, which does not bear the ISCR-*cat* insertion (Fig. 2). Since pAsa4 carries those two regions, A449 is resistant to both antibiotics.

290

291

292 Among a collection of *A. salmonicida* subsp. *salmonicida* from Canada and Europe, 11 isolates
293 (A449 included) were detected with pAsa4-positive PCR genotyping results using a single pair
294 of primers (Table 1, Table S2). These isolates had different resistance profiles for tetracycline,
295 chloramphenicol and sulfamethoxazole-trimetoprim (SXT) resistance, and no one was resistant
296 to florfenicol, another aquaculture-relevant antibiotic whose resistance is conferred by pSN254b
297 (Table 1, Table S1). 01-B522 was the only SXT-resistant strain, and since only the
298 sulphonamides resistance is encoded on pAsa4, 01-B522 genome has another element to provide
299 trimethoprim resistance. Otherwise, strains bearing pAsa4 variants could be clustered in three
300 groups: tetracycline resistant, chloramphenicol resistant and resistant to both antibiotics.

301

302 We refined our genotyping of the pAsa4 variants by designing primers covering each segment
303 junction (Fig. 1B, Table S2). All 11 pAsa4-positive isolates were associated with one variant
304 version: pAsa4, pAsa4b, or pAsa4c (Table 1). All but one of the isolates (RS 1458) displayed the
305 junction pattern (Fig. 1B) of their variant type and had a concordant antibiotic resistance profile
306 (Table 1). The irregular strain RS 1458 had a pAsa4b pattern, except for Tn*21* (Fig. 1B, yellow
307 to green junction). With exception of the two strains of unknown geographic origin, pAsa4b was
308 found in Canada, while pAsa4 and pAsa4c were found in Europe (Table 1).

Discussion

pAsa4 is a large antimicrobial resistance-carrying plasmid that was sequenced with *A. salmonicida* subsp. *salmonicida* reference genome (Reith et al. 2008). In this study, we characterized two pAsa4 variants, pAsa4b and pAsa4c. The analysis of these variants highlighted the importance of mobile genetic elements in shaping the genomic landscape of this bacterium, in particular its antibiotic resistance and, potentially, its ability to disseminate antibiotic resistance by conjugation. Moreover, comparative genomics between variants and other plasmids as well as base substitution analysis were used to infer pAsa4 modular architecture.

The variable position of the ISs in the pAsa4 variants indicated that they were active and capable of transposition (Fig. 1A). Among all the ISs found in pAsa4 variants, the Tn*21*-disrupted IS*AS5* is the only one to be at the same position in every plasmid. These evidences are additional examples of IS activity responsible for plasmid variations in *A. salmonicida* subsp. *salmonicida* (Attere et al. 2015; Najimi et al. 2009; Trudel et al. 2013; Vincent et al. 2014b). Moreover, pAsa4c bears IS*Knp3*, originally described on *Klebsiella pneumoniae* plasmid pRDDHA. Based on its transposase annotation, up to twelve copies of this IS could be found in the *Aeromonas media* WS chromosome (accession number CP007567) and 1 to 3 copies could be found in *Aeromonas dhakensis* SSU (accession number JDWD00000000.1). However, *A. media* WS may be prone to "infection" by ISs since it bears 326 transposase-associated annotations. This may not be representative of the distribution of this IS in the *Aeromonas* genus (Chai et al. 2012; Vincent et al. 2016). All these ISs can disrupt genes and functions by subsequent transposition, or can be targeted by the recombination machinery to produce larger structural variations, and thus bring a genetic modification potential. In pAsa4, two IS*AS1*s could be used to mediate the

inversion (Fig. 1A). Similar IS-dependent recombinations have been observed in pAsa5 variants in *A. salmonicida* subsp. *salmonicida* and have been reproduced *in vitro* by growing the bacteria under stressful conditions (Daher et al. 2011; Emond-Rheault et al. 2015; Tanaka et al. 2012; Vincent et al. 2016).

Architectural differences between pAsa4 variants, both mobile element-mediated or not, affected functions. Large-scale recombinations and insertions/deletions also had an impact on the number and orientation of conjugative transfer genes. pAsa4b had the most complete version of the large conjugative region compared to previously described gene repertoires (Nonaka et al. 2014) (Fig. 1B, rainbow segments). In this case, pAsa4b bears the same number and synteny of coding sequences that plasmids known to propagate by conjugation (Fernandez-Alarcon et al. 2011). However, the ability to propagate by conjugation cannot be inferred exclusively by *in silico* analysis since it can be influenced by point mutations (Call et al. 2010).

In*2* is both an active mobile element in pAsa4 and a site for complex IS integration. The cassette integration system is potentially active given the presence of *aadA* cassette in pAsa4 and pAsa4c. This region also contained the *cat* gene, encoding a chloramphenicol acetyltransferase, which was not integrated as a cassette, but rather by an IS*CR*-like insertion sequence (Fig. 2). This provides another example of phenotypic diversity driven by ISs. The IS*CR* elements, which are known to transpose *cis* resistance genes between class 1 integrons in non-standard transpositions, may also create integron fragment duplications during those events (Toleman et al. 2006). In pAsa4, the duplication of the integrase between the IS*CR* transposase fragment and the cassette structure is an indication of a complex transposition.

Empirical segments representing insertion/deletion and inversion were created to facilitate comprehension and genotyping of the pAsa4 variants. PCR across the segments junctions paired with antimicrobial disk assay assigned plasmid variant types to strains that bore pAsa4-like plasmids (Table 1). However, such clustering did not always adequately represent plasmid modules, that is, genes of common function or origin. For instance, Tn*21* spawns across three segments in Fig. 1B. Thus, base substitution counts (Fig. S1) and tBlastn comparisons (Fig. 3) were used to further our analysis. The heatmap and the resulting clustering revealed previously observed similarities between pAsa4 and the IncA/C incompatibility group (Fricke et al. 2009). However, two pAsa4b regions were poorly covered by hits in this analysis. One was the region deleted in pAsa4c, corresponding to blue segment in Fig. 1B. In that case, this region is a module that could bring specific accessory functions to pAsa4-bearing strains. The other region poorly covered by hits was a region immediately downstream from Tn*21*. Interestingly, the base substitution analysis also showed that this region was not prone to mutation. This region contains many genes that code for hypothetical proteins, thus their implication in pAsa4 maintenance or functions are unknown. However, given their presence in all variants and the region low substitution rate, it could contain genes essential for pAsa4 maintenance.

pSN254b is another large, antimicrobial resistance genes-carrying plasmid found in many Canadian *A. salmonicida* subsp. *salmonicida* isolates (McIntosh et al. 2008; Vincent et al. 2014b). When compared together, pAsa4b and pSN254b showed similarities as well as synteny. This alignment revealed that pAsa4 indeed possesses some specific regions, here Fig. 1B blue segment, Tn*21* downstream region, but also Tn*21* upstream region.

379

380 # Conclusion and Perspectives

381 Our results showed that pAsa4 variant architecture impacted on resistance antibiotic genes, and
382 identified active ISs and integration hotspots that could promote novel resistances combinations.
383 Because of its ubiquitous nature, *A. salmonicida* subsp. *salmonicida* interacts with many other
384 waterborne microbes. Therefore, it may serve as a reservoir for disseminating new plasmid-based
385 combinations of antimicrobial resistance. Even if pAsa4 was not as prevalent as pSN254b in
386 geographic regions included in the present study, it should be regarded as a potential threat to the
387 propagation and shuffling of antibiotic resistance due to its modular and recombinant structure.
388 The transmission of pAsa4 should thus be monitored, especially given the propagation of *A.*
389 *salmonicida* subsp. *salmonicida* infections in fish farms.

390

Acknowledgments

We thank Mathilde Goldschmitt for technical support. We also thank the Laboratoire de bactériologie clinique, Faculté de médecine vétérinaire, Université de Montréal (Montreal, QC, Canada), the Félix d'Hérelle Reference Center (Département de biochimie, de microbiologie et de bio-informatique, Université Laval, Quebec City, QC, Canada) as well as M. Reith (National Research Council laboratories, Halifax, Nova Scotia), J. Frey (University of Bern), and R.M.W. Stevenson (University of Guelph) for the *A. salmonicida* subsp. *salmonicida* isolates.

400 # References

401

402 Altschul SF, Gish W, Miller W, Myers EW, and Lipman DJ. 1990. Basic local alignment search
403 tool. *Journal of Molecular Biology* 215:403-410. 10.1016/s0022-2836(05)80360-2
404 Attere SA, Vincent AT, Trudel MV, Chanut R, and Charette SJ. 2015. Diversity and
405 Homogeneity among Small Plasmids of *Aeromonas salmonicida* subsp. *salmonicida*
406 Linked with Geographical Origin. *Front Microbiol* 6:1274. 10.3389/fmicb.2015.01274
407 Call DR, Singer RS, Meng D, Broschat SL, Orfe LH, Anderson JM, Herndon DR, Kappmeyer
408 LS, Daniels JB, and Besser TE. 2010. *bla*CMY-2-positive IncA/C plasmids from
409 *Escherichia coli* and *Salmonella enterica* are a distinct component of a larger lineage of
410 plasmids. *Antimicrobial Agents and Chemotherapy* 54:590-596. 10.1128/AAC.00055-09
411 Chai B, Wang H, and Chen X. 2012. Draft genome sequence of high-melanin-yielding
412 *Aeromonas media* strain WS. *Journal of Bacteriology* 194:6693-6694.
413 10.1128/JB.01807-12
414 Daher RK, Filion G, Tan SG, Dallaire-Dufresne S, Paquet VE, and Charette SJ. 2011. Alteration
415 of virulence factors and rearrangement of pAsa5 plasmid caused by the growth of
416 *Aeromonas salmonicida* in stressful conditions. *Veterinary Microbiology* 152:353-360.
417 S0378-1135(11)00264-1 [pii]10.1016/j.vetmic.2011.04.034
418 Dallaire-Dufresne S, Tanaka KH, Trudel MV, Lafaille A, and Charette SJ. 2014. Virulence,
419 genomic features, and plasticity of *Aeromonas salmonicida* subsp. *salmonicida*, the
420 causative agent of fish furunculosis. *Veterinary Microbiology* 169:1-7.
421 10.1016/j.vetmic.2013.06.025

422 Derome N, Boutin S, Llewellyn M, and Gauthier J. 2016. Opportunistic pathogens of fish. In:
423 Hurst CJ, ed. *The Rasputin effect: when commensals and symbionts become parasitic*.
424 New York, NY: Springer, 649.
425 Emond-Rheault JG, Vincent AT, Trudel MV, Frey J, Frenette M, and Charette SJ. 2015.
426 AsaGEI2b: a new variant of a genomic island identified in the *Aeromonas salmonicida*
427 subsp. *salmonicida* JF3224 strain isolated from a wild fish in Switzerland. *FEMS*
428 *Microbiology Letters* 362. 10.1093/femsle/fnv093
429 Fernandes F, da Fonseca PG, Russo LM, Oliveira AL, and Freitas AT. 2011. Efficient alignment
430 of pyrosequencing reads for re-sequencing applications. *BMC Bioinformatics* 12:163.
431 10.1186/1471-2105-12-163
432 Fernandez-Alarcon C, Singer RS, and Johnson TJ. 2011. Comparative genomics of multidrug
433 resistance-encoding IncA/C plasmids from commensal and pathogenic *Escherichia coli*
434 from multiple animal sources. *PLoS One* 6:e23415. 10.1371/journal.pone.0023415
435 Fricke WF, Welch TJ, McDermott PF, Mammel MK, LeClerc JE, White DG, Cebula TA, and
436 Ravel J. 2009. Comparative genomics of the IncA/C multidrug resistance plasmid family.
437 *Journal of Bacteriology* 191:4750-4757. 10.1128/JB.00189-09
438 Galardini M, Biondi EG, Bazzicalupo M, and Mengoni A. 2011. CONTIGuator: a bacterial
439 genomes finishing tool for structural insights on draft genomes. *Source Code Biol Med*
440 6:11. 10.1186/1751-0473-6-11
441 Garcia-Alcalde F, Okonechnikov K, Carbonell J, Cruz LM, Gotz S, Tarazona S, Dopazo J,
442 Meyer TF, and Conesa A. 2012. Qualimap: evaluating next-generation sequencing
443 alignment data. *Bioinformatics* 28:2678-2679. 10.1093/bioinformatics/bts503

444 Gordon D, and Green P. 2013. Consed: a graphical editor for next-generation sequencing.
445 *Bioinformatics* 29:2936-2937. 10.1093/bioinformatics/btt515
446 Gustafson CE, Chu SJ, and Trust TJ. 1994. Mutagenesis of the paracrystalline surface protein
447 array of *Aeromonas salmonicida* by endogenous insertion elements. *Journal of Molecular*
448 *Biology* 237:452-463. 10.1006/jmbi.1994.1247
449 Hanninen ML, and Hirvela-Koski V. 1997. Molecular and phenotypic methods for the
450 characterization of atypical *Aeromonas salmonicida*. *Veterinary Microbiology* 56:147-
451 158. 10.1016/S0378-1135(96)01339-9
452 Harmer CJ, and Hall RM. 2015. The A to Z of A/C plasmids. *Plasmid* 80:63-82.
453 10.1016/j.plasmid.2015.04.003
454 Hartigan JA, and Wong MA. 1979. Algorithm AS 136: A K-Means Clustering Algorithm.
455 *Journal of the Royal Statistical Society Series C (Applied Statistics)* 28:100-108.
456 10.2307/2346830
457 Liebert CA, Hall RM, and Summers AO. 1999. Transposon Tn*21*, flagship of the floating
458 genome. *Microbiology and Molecular Biology Reviews* 63:507-522.
459 Margulies M, Egholm M, Altman WE, Attiya S, Bader JS, Bemben LA, Berka J, Braverman
460 MS, Chen YJ, Chen Z, Dewell SB, Du L, Fierro JM, Gomes XV, Godwin BC, He W,
461 Helgesen S, Ho CH, Irzyk GP, Jando SC, Alenquer ML, Jarvie TP, Jirage KB, Kim JB,
462 Knight JR, Lanza JR, Leamon JH, Lefkowitz SM, Lei M, Li J, Lohman KL, Lu H,
463 Makhijani VB, McDade KE, McKenna MP, Myers EW, Nickerson E, Nobile JR, Plant R,
464 Puc BP, Ronan MT, Roth GT, Sarkis GJ, Simons JF, Simpson JW, Srinivasan M, Tartaro
465 KR, Tomasz A, Vogt KA, Volkmer GA, Wang SH, Wang Y, Weiner MP, Yu P, Begley

RF, and Rothberg JM. 2005. Genome sequencing in microfabricated high-density picolitre reactors. *Nature* 437:376-380. 10.1038/nature03959

McArthur AG, Waglechner N, Nizam F, Yan A, Azad MA, Baylay AJ, Bhullar K, Canova MJ, De Pascale G, Ejim L, Kalan L, King AM, Koteva K, Morar M, Mulvey MR, O'Brien JS, Pawlowski AC, Piddock LJ, Spanogiannopoulos P, Sutherland AD, Tang I, Taylor PL, Thaker M, Wang W, Yan M, Yu T, and Wright GD. 2013. The comprehensive antibiotic resistance database. *Antimicrobial Agents and Chemotherapy* 57:3348-3357. AAC.00419-13 [pii]

10.1128/AAC.00419-13

McIntosh D, Cunningham M, Ji B, Fekete FA, Parry EM, Clark SE, Zalinger ZB, Gilg IC, Danner GR, Johnson KA, Beattie M, and Ritchie R. 2008. Transferable, multiple antibiotic and mercury resistance in Atlantic Canadian isolates of *Aeromonas salmonicida* subsp. *salmonicida* is associated with carriage of an IncA/C plasmid similar to the *Salmonella enterica* plasmid pSN254. *Journal of Antimicrobial Chemotherapy* 61:1221-1228. Doi 10.1093/Jac/Dkn123

Morin R. 2010. L'utilisation des antibiotiques pour combattre la furonculose chez l'omble de fontaine génère de l'antibiorésistance chez *Aeromonas salmonicida*. *L'Aquicole - Le Bulletin de l'Association des aquaculteurs du Québec* 15.

Najimi M, Balado M, Lemos ML, and Osorio CR. 2009. Genetic characterization of pAsa6, a new plasmid from *Aeromonas salmonicida* subsp. *salmonicida* that encodes a type III effector protein AopH homolog. *Plasmid* 61:176-181. S0147-619X(09)00002-X [pii]10.1016/j.plasmid.2009.01.001

Nonaka L, Maruyama F, Onishi Y, Kobayashi T, Ogura Y, Hayashi T, Suzuki S, and Masuda M. 2014. Various pAQU plasmids possibly contribute to disseminate tetracycline resistance gene *tet*(M) among marine bacterial community. *Front Microbiol* 5:152. 10.3389/fmicb.2014.00152

Pearson WR, and Lipman DJ. 1988. Improved tools for biological sequence comparison. *Proceedings of the National Academy of Sciences of the United States of America* 85:2444-2448.

Piotrowska M, and Popowska M. 2015. Insight into the mobilome of *Aeromonas* strains. *Front Microbiol* 6:494. 10.3389/fmicb.2015.00494

R Core Team. 2015. R: A Language and Environment for Statistical Computing. Vienna, Austria: R Foundation for Statistical Computing.

Ramirez MS, and Tolmasky ME. 2010. Aminoglycoside modifying enzymes. *Drug Resist Updat* 13:151-171. 10.1016/j.drup.2010.08.003

Reith ME, Singh RK, Curtis B, Boyd JM, Bouevitch A, Kimball J, Munholland J, Murphy C, Sarty D, Williams J, Nash JH, Johnson SC, and Brown LL. 2008. The genome of *Aeromonas salmonicida* subsp. *salmonicida* A449: insights into the evolution of a fish pathogen. *BMC Genomics* 9:427. 10.1186/1471-2164-9-427

Rice P, Longden I, and Bleasby A. 2000. EMBOSS: the European Molecular Biology Open Software Suite. *Trends in Genetics* 16:276-277.

Rutherford K, Parkhill J, Crook J, Horsnell T, Rice P, Rajandream MA, and Barrell B. 2000. Artemis: sequence visualization and annotation. *Bioinformatics* 16:944-945.

509 Siguier P, Perochon J, Lestrade L, Mahillon J, and Chandler M. 2006. ISfinder: the reference
510 centre for bacterial insertion sequences. *Nucleic Acids Res* 34:D32-36.
511 10.1093/nar/gkj014
512 Sorum H, L'Abee-Lund T, Solberg A, and Wold A. 2003. Integron-containing IncU R plasmids
513 pRAS1 and pAr-32 from the fish pathogen *Aeromonas salmonicida*. *Antimicrobial*
514 *Agents and Chemotherapy* 47:1285-1290. Doi 10.1128/aac.47.4.1285-1290.2003
515 Studer N, Frey J, and Vanden Bergh P. 2013. Clustering subspecies of *Aeromonas salmonicida*
516 using IS*630* typing. *BMC Microbiol* 13:36. 10.1186/1471-2180-13-36
517 Sullivan MJ, Petty NK, and Beatson SA. 2011. Easyfig: a genome comparison visualizer.
518 *Bioinformatics* 27:1009-1010. 10.1093/bioinformatics/btr039
519 Tanaka KH, Dallaire-Dufresne S, Daher RK, Frenette M, and Charette SJ. 2012. An insertion
520 sequence-dependent plasmid rearrangement in *Aeromonas salmonicida* causes the loss of
521 the type three secretion system. *PLoS One* 7:e33725. 10.1371/journal.pone.0033725
522 Tanaka KH, Frenette M, and Charette SJ. 2013. IS-mediated loss of virulence by *Aeromonas*
523 *salmonicida*: A tangible piece of an evolutionary puzzle. *Mob Genet Elements* 3:e23498.
524 10.4161/mge.23498
525 Toleman MA, Bennett PM, and Walsh TR. 2006. Common regions e.g. orf*513* and antibiotic
526 resistance: IS*91*-like elements evolving complex class 1 integrons. *Journal of*
527 *Antimicrobial Chemotherapy* 58:1-6. 10.1093/jac/dkl204
528 Trudel MV, Tanaka KH, Filion G, Daher RK, Frenette M, and Charette SJ. 2013. Insertion
529 sequence *AS5* (IS*AS5*) is involved in the genomic plasticity of *Aeromonas salmonicida*.
530 *Mob Genet Elements* 3:e25640. 10.4161/mge.25640

Verdet C, Benzerara Y, Gautier V, Adam O, Ould-Hocine Z, and Arlet G. 2006. Emergence of DHA-1-producing *Klebsiella spp*. in the Parisian region: genetic organization of the *ampC* and *ampR* genes originating from *Morganella morganii*. *Antimicrobial Agents and Chemotherapy* 50:607-617. 10.1128/AAC.50.2.607-617.2006

Vincent AT, Boyle B, Derome N, and Charette SJ. 2014a. Improvement in the DNA sequencing of genomes bearing long repeated elements. *Journal of Microbiological Methods* 107:186-188. 10.1016/j.mimet.2014.10.016

Vincent AT, Trudel MV, Freschi L, Nagar V, Gagne-Thivierge C, Levesque RC, and Charette SJ. 2016. Increasing genomic diversity and evidence of constrained lifestyle evolution due to insertion sequences in *Aeromonas salmonicida*. *BMC Genomics* 17:44. 10.1186/s12864-016-2381-3

Vincent AT, Trudel MV, Paquet VE, Boyle B, Tanaka KH, Dallaire-Dufresne S, Daher RK, Frenette M, Derome N, and Charette SJ. 2014b. Detection of variants of the pRAS3, pAB5S9, and pSN254 plasmids in *Aeromonas salmonicida* subsp. *salmonicida*: multidrug resistance, interspecies exchanges, and plasmid reshaping. *Antimicrobial Agents and Chemotherapy* 58:7367-7374. 10.1128/AAC.03730-14

Wickham H. 2009. *ggplot2: elegant graphics for data analysis*: Springer New York.

Ye J, Coulouris G, Zaretskaya I, Cutcutache I, Rozen S, and Madden TL. 2012. Primer-BLAST: a tool to design target-specific primers for polymerase chain reaction. *BMC Bioinformatics* 13:134. 10.1186/1471-2105-13-134

Zeileis A, and Grothendieck G. 2005. zoo: S3 Infrastructure for Regular and Irregular Time Series. *Journal of Statistical Software* 14:1-27.

554

1

Nucleotide alignment of three plasmid variants: pAsa4, pAsa4b, and pAsa4c.

(a) The three linear representations were aligned and visualized using EasyFig (Sullivan et al. 2011) . The dark grey bands denote regions of identity. Overall, the identity was more than 94%. The bands of non-contiguous repeat regions were removed for clarity. An inversion between pAsa4 and pAsa4b/c is marked in orange. Open reading frames (ORFs) are indicated by colored arrows that indicate their deduced function: **Cyan:** hypothetical protein; **Dark grey:** maintenance and replication; **Blue**: type IV secretion system-like conjugative system, contained in two conjugative blocks (dashed lines); **Red**: insertion sequence, transposition-associated genes; **Orange:** antimicrobial resistance. The following features have also been annotated: **Asterisk:** IS*AS2* and acetyltransferase insertion in pAsa4c; **Dagger:** IS*1595*-family IS*Kpn3*. A transposon/integron structure (Tn*21*/In*2*) that was common to all pAsa4 plasmids and that is integrated into an IS*AS5* is indicated over each plasmid by nested red, green, and yellow arrows. Besides the transposon, but inside IS*AS5*, an IS*AS9* and an IS*AS2* insertion could be seen for pAsa4 and pAsa4c, respectively. (**b)** Segments of large insertion/deletion or recombination sequences are highlighted in color. Segments of particular significance are: **Blue**: an insertion/deletion in pAsa4 comprising tetracycline resistance genes *tetAR*(E); **Rainbow**: multiple insertions/deletions and an inversion encompassing a conjugative gene region; **Pink**: two events: an IS*CR* insertion comprising the chloramphenicol resistance gene *cat* and a *aadA1* cassette.

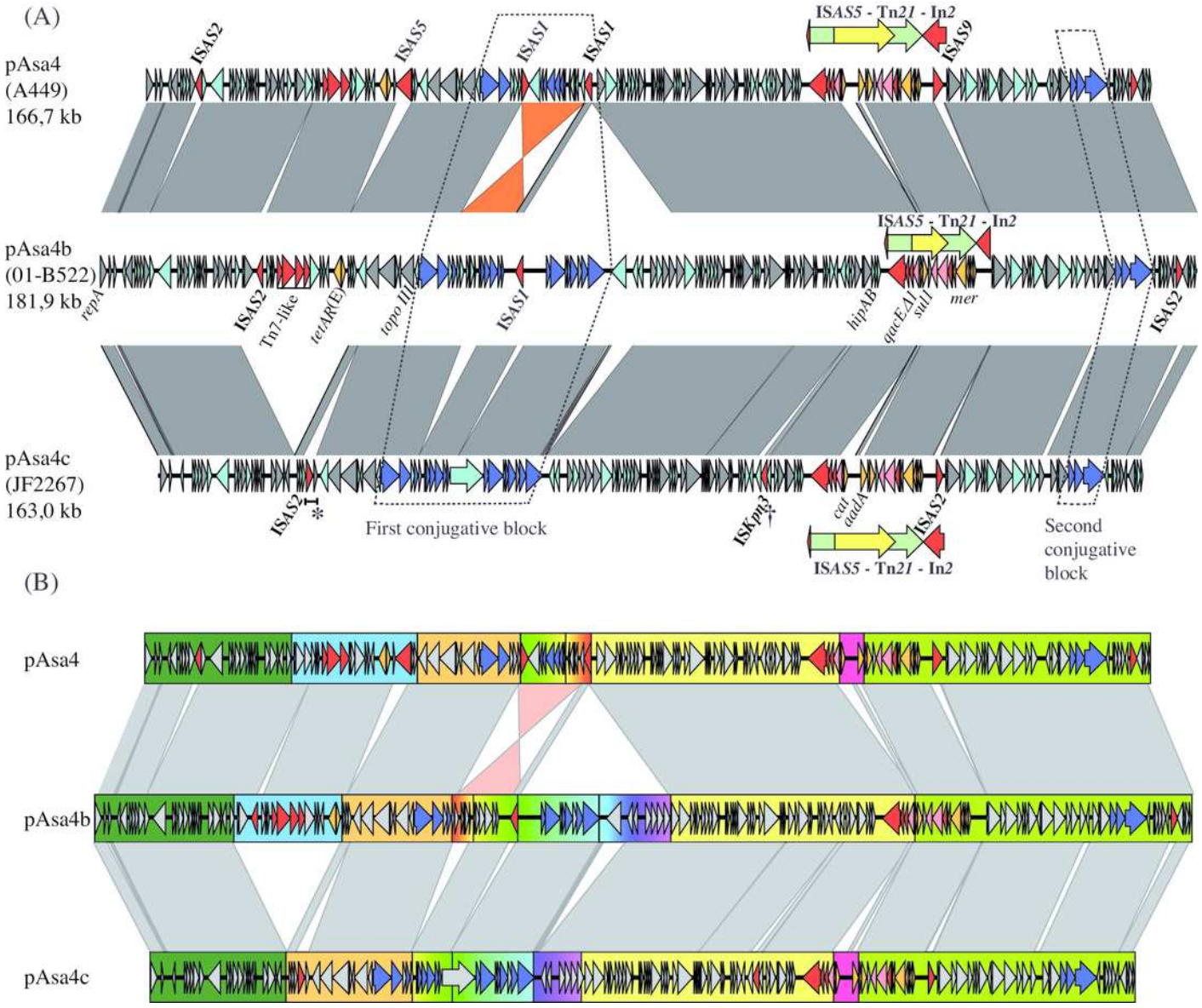

2

In*2* comparison between pAsa4b and the other variants.

Tn*21* differences between the variants are all located in In*2*. Features are colored using the following: **Red:** Tn*21* transposition genes, **Pink**: In*2* integrase, transposition features and insertion sites, **Cyan**: hypothetical proteins, **Orange**: Antibiotic and mercury resistance genes, **Green**: IS*CR*-related features. Two doted rectangles represent a repeat region in pAsa4/pAsa4c In*2*, likely caused by *cat*-IS*CR* insertion. This IS is partial, lacking a *terIS* and part of its transposase, suggesting a complex insertion event.

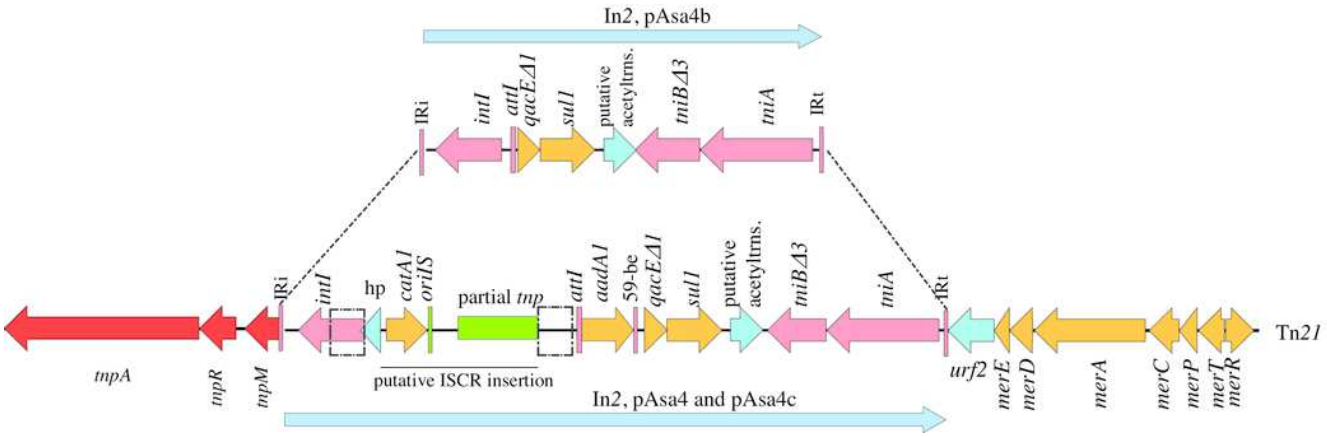

3

Clustering tBlastn results for pAsa4b.

The shading denotes the maximum identity between the ORF query and the target. *k-means* clustered the molecules into four stable groups: Group 1 a and b is representative of incompatibility group IncA/C plasmids; Groups 2 and 4 do not encompass a specific type of sequence identifiers. However, Group 2 shares significant identity with Tn*21* targets; Group 3 is representative of integrative and conjugative elements (ICEs). Some regions are less covered by tBlastn hits, such as Fig. 1B blue segment, and a region downstream from Tn*21*.

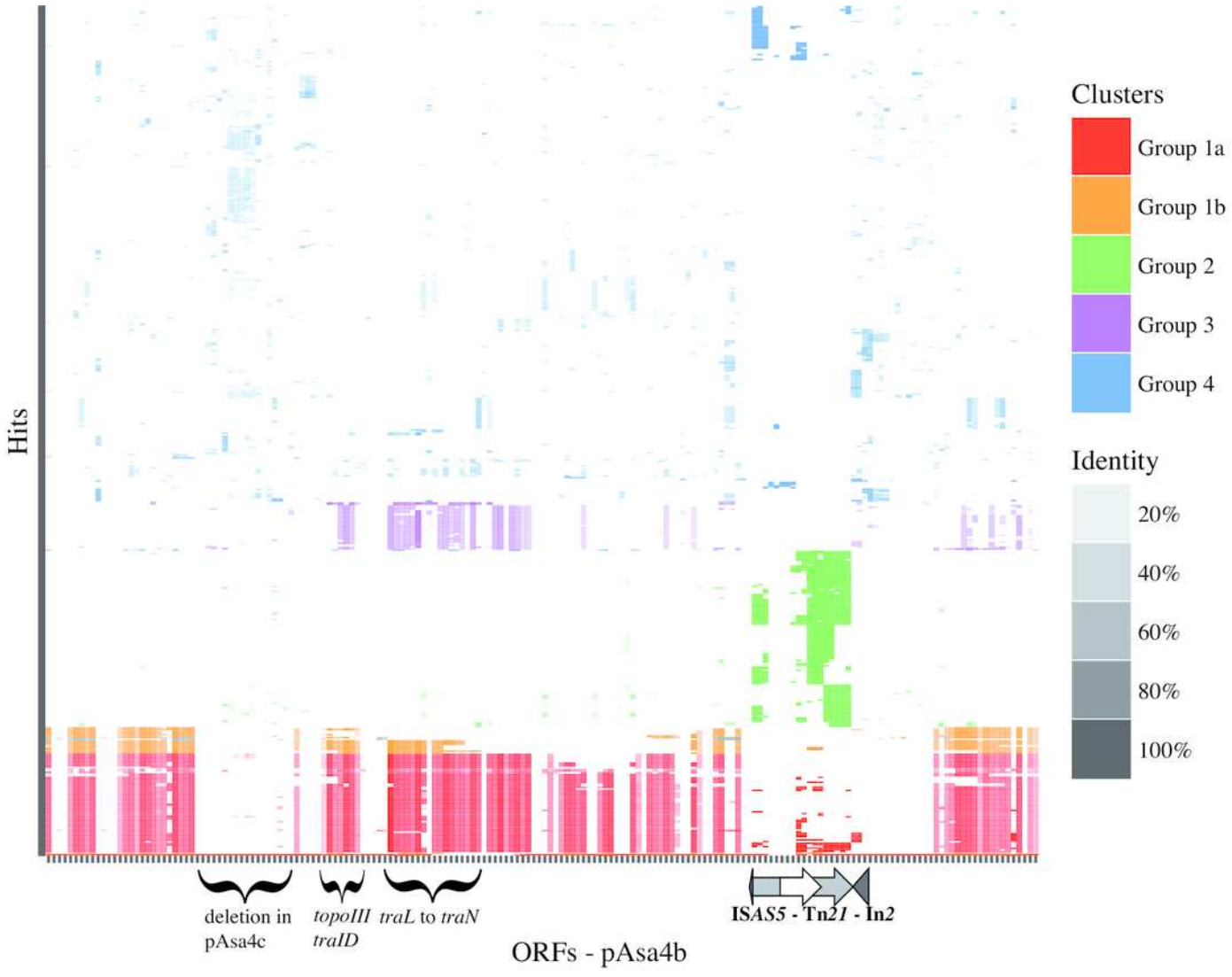

4

Nucleotide alignment between pAsa4b and pSN254b.

The linear representations were aligned and visualized using EasyFig (Sullivan et al. 2011) .

The color codes and segments are the same as in Fig 1.

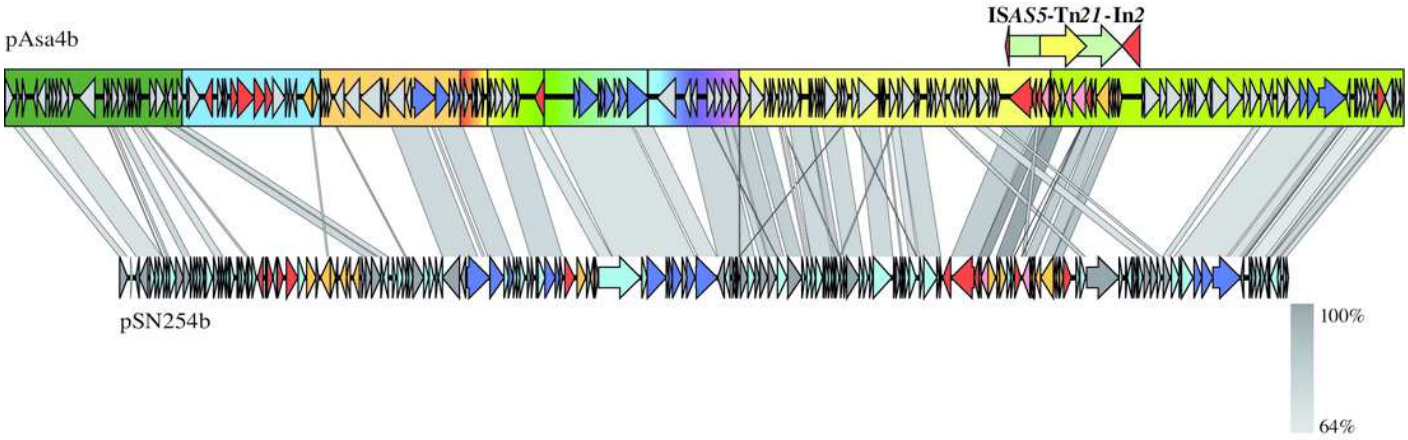

Table 1(on next page)

A. salmonicida subsp. *salmonicida* strains bearing pAsa4 variants.

1

Strain	Origin*	Antibiotic resistance determined by antibiogram†	pAsa4 variant determined by genotyping	Reference
A449	France	TET, CHL	pAsa4	(Reith et al. 2008)
RS 534 (A450)	France	TET, CHL	pAsa4	(Kay et al. 1981)
01-B522	Quebec (Canada)	SXT, TET	pAsa4b	(Daher et al. 2011)
RS 1458	Ontario (Canada)	TET	pAsa4b	(Attere et al. 2015)
SHY13-2627	Quebec (Canada)	TET	pAsa4b	(Attere et al. 2015)
SHY13-3799	Quebec (Canada)	TET	pAsa4b	(Attere et al. 2015)
HER1107	INA	TET	pAsa4b	(Daher et al. 2011)
JF2267	Switzerland	CHL	pAsa4c	(Braun et al. 2002)
JF3517	Norway	CHL	pAsa4c	(Burr & Frey 2007)
JF3518	Norway	CHL	pAsa4c	(Burr & Frey 2007)
JF2869	INA	CHL	pAsa4c	(Studer et al. 2013)

2 *INA: Information not available or not traceable

3 †SXT = sulfamethoxazole/trimethoprim, TET = tetracycline, CHL = chloramphenicol

4